Journal of Solid Mechanics Vol. 14, No. 4 (2022) pp. 418-429
DOI: 10.22034/jsm.2021.1891483.1540

Research Paper

Experimental and Numerical Investigations of the Effect of Impact Angle and Impactor Geometry on the High-Velocity Impact Response of Aluminum Honeycomb Structures

H. Alikhani [1], S. Derakhshan [2], H. Khoramishad [1,*]

[1]*School of Mechanical Engineering, Iran University of Science & Technology (IUST), Narmak, Tehran 16846-13114, Iran*
[2]*School of Mechanical Engineering, Amirkabir University of Technology, Tehran, Iran*

Received 30 June 2022; accepted 31August 2022

ABSTRACT

In this study, the effects of impact angle and impactor geometry were investigated on the impact behavior of aluminum honeycombs experimentally and numerically. The high-velocity impact tests were carried out using a gas-gun test machine with flat, spherical and conical-head impactors and impact angles of 0°, 15° and 30° at different incident velocities ranging from 55.8 to 150.5 m/s. The numerical models were developed in LS-Dyna finite element code and well validated against the experimental results. The results showed that the impact behavior of honeycombs is considerably dependent on the impactor head geometry and the impact angle. The honeycomb panel impacted by the conical projectile experienced the highest absorbed energy and ballistic limit velocity. Moreover, it was found out that increasing the impact angle increased the absorbed energy and ballistic limit velocity of honeycombs. Furthermore, different impactor head geometries resulted in different failure mechanisms in the course of impact loading.

Keywords : Aluminum honeycomb; High-velocity impact; Energy absorption; Impactor geometry; Impact angle.

1 INTRODUCTION

HONEYCOMB structures were introduced almost fifty years ago and found important applications in different industries. Many studies have been carried out on the mechanical properties of honeycombs. However, due to the complicated behavior of honeycomb structures, most of the studies have been dedicated to experimental observations. Honeycomb structures have found wide applications in sandwich and energy absorbent systems

*Corresponding author. Tel.: +98 2177240540-50; Fax: +98 2177240488.
E-mail address: Khoramishad@iust.ac.ir (H. Khoramishad)

because of their high energy absorption capability and shock absorbance. Honeycombs as cellular structures with very low weight have high strength and energy absorption to weight ratios. Due to their anisotropic behavior, when a honeycomb structure is impacted, it can present different energy absorption behaviors in different directions [1-2]. Zhou and Mayer [3] found that the out-of-plane strength of honeycombs was approximately two times higher than their in-plane strengths. Honeycomb structures may have different cellular shapes such as square, triangular, diamond and hexagonal thus they can provide different advantages. For example, a honeycomb with square cells has a higher impact resistance compared to the honeycomb structures with hexagonal cells. As a result, the honeycomb structures with square cells can be used as stiff materials such as stainless steel [4]. Many researchers (e.g. [5-8]) have experimentally studied the effect of geometrical and material parameters on the impact behavior of honeycomb structures. The impact tests of honeycombs are usually carried out using the gas-gun, drop weight machine and Hopkinson pressure bar [9]. Zhao and Gary [10] investigated the impact behavior of honeycombs using the Hopkinson pressure bar. They concluded that the strength of honeycombs in T-direction has a direct relationship with the honeycomb density. They showed that the compressive strength of honeycombs in this direction depended on the loading rate. Therefore, the strength of honeycombs under high strain rates was 40% more than that under static loading. Baker and Togami [11] proposed a special instrument based on the gas-gun machine and provided high-velocity impact tests on honeycombs. They illustrated that the mechanical behavior of honeycombs depended on the strain rate and found out that the dynamic peal strength was 50% higher than the quasi-static strength. This difference between the dynamic and quasi-static responses of honeycomb structures was attributed to their different local collapse modes under dynamic and quasi-static loadings. Liaghat and Alavi Nia [12] investigated different parameters influencing the high-velocity impact behavior of honeycombs and found out that the overall structure thickness, the shear yield strength and the wall thickness had direct effects and the cell size and the mass of impactor had inverse effects on the honeycomb resistance against impactor penetration. These findings were confirmed by He and Yao [13] and Guan and Liu [14] for the low-velocity impact behavior of honeycomb structures by conducting experimental and numerical studies. Yamashita and Gotoh [15] experimentally investigated the effect of cell angle and wall thickness on the collapse mechanisms of honeycombs made of aluminum 5052. Moreover, they numerically studied the effect of the wall angles by varying it from 30° to 180° on the honeycomb strength and reported the higher crush strength for the wall angle of 120°. Wu et al. [16] investigated the effect of the impact energy and the overall structure thickness on the impact behavior of a honeycomb sandwich beam experimentally. They showed that increasing the structure thickness increased the structure resistance against impact loading. On the other hand, 50% of impact energy was absorbed by the honeycomb core indicating the dominant role of the honeycomb core in the energy absorption capability of sandwich structures. There are several researchers [17-20] worked on the numerical modeling of high-velocity and low-velocity impact responses of honeycombs to identify the micro and macro energy absorption mechanisms that were not visible and measurable by merely experimental testing. Aktay and Johnson [21] employed the micro-scale and homogenized finite element models and compared the results of the experimental and numerical studies. They concluded that the micro-scale model was more appropriate for honeycombs due to the higher accuracy it can provide. Li and et al. [22] studied numerically and analytically the strain rate sensitivity of hexagonal honeycombs by testing under out-of-plan impact loading. They showed that initiation of bucklewaves caused buckling and folding of cell walls. Appearance of these damage mechanisms led to short peak stress plateau which was followed by prolonged crushing stress plateau.

In this paper, the effect of two parameters including the impactor geometry and the impact angle on the high-velocity impact response of honeycombs was studied experimentally and numerically. The impactor geometries of flat, spherical and conical and the impact angles of 0°, 15° and 30° were considered. The LS-DYNA finite element code was employed for numerical investigations. The finite element models were validated against the experimental gas-gun test results. The energy absorption and the ballistic limit were considered as the main high-velocity responses of the honeycomb structure. Moreover, the contact surface between the projectile and honeycomb and the projectile penetration time and the damaged area of honeycomb were assessed in the course of impact loading.

2 EXPERIMANTAL STUDY

2.1 Materials and methods

The honeycomb panels were made of aluminum 1110 with a thickness of 50 μm. The honeycomb cells were hexagonal with a size of 4 mm and an overall panel thickness of 10 mm. The mechanical properties of aluminum 1110 were obtained as presented in Table 1. The dimensions of the honeycomb panels were $120\times120\times10$ mm^3 due to the gas-gun fixture requirements.

Table 1
The mechanical properties of aluminum 1110.

Tensile strength (*MPa*)	Poisson's ratio	Shear modulus (*GPa*)	Elastic modulus (*GPa*)
276	0.33	26	69

Two sets of experimental tests were conducted on the honeycomb panels. As the first experimental tests set, the high-velocity impact tests were conducted on the honeycomb panels with different impactor geometries of flat, spherical and conical and at an impact angle of θ=0° (vertical impact). As the second experimental tests set, the high velocity impact tests were performed on the honeycomb panels at different impact angles of θ=0°, θ=15° and θ=30° and with an impactor geometry of flat. Fig. 1 shows the different projectile geometries and the honeycomb structure considered for experimental tests.

The impactors were made of steel ST37 with three different head geometries of flat, spherical and conical. The flat-head impactor had a diameter of 6 *mm* and a length of 16 *mm* (length to diameter ratio=2) and for the spherical-head impactor, the length of the cylindrical part and the diameter of the spherical part were 15 *mm* and 6 *mm*, respectively. The cone angle of the conical-head impactor was 60° and the length and diameter of the cylindrical part were 12.8 *mm* and 6 *mm*, respectively. The masses of projectiles for three different head geometries of flat, spherical and conical were 6.937, 6.20 and 5.274 *gr*, respectively. To fix the honeycomb panel at inclined positions a fixture was designed which was made of two steel plates with the dimensions of 145×125×10 mm^3 and a hollow square in the central part with the dimensions of 70×70 mm^2. The plates were clamped using four M12 bolts and the target was placed between the two steel plates. In order to adjust the impact angles of 15° and 30°, wedges with precise angles of θ=15° and θ=30° were placed under the fixture. The test setup of the high-velocity impact tests is shown in Fig. 2. The velocity of impactor was measured using a laser-based device with two laser lines. When the impactor passed through the lines with a known distance, the time was recorded and based on the distance between the two lines, the residual velocity was calculated.

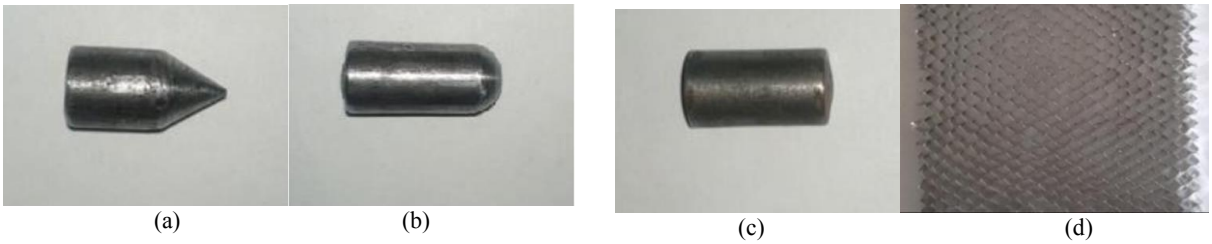

(a) (b) (c) (d)

Fig.1
The impactors used for experimental tests (a) Conical-head (b) Spherical-head (c) Flat head (d) Honeycomb structure used for experimental tests.

Fig.2
Test setup of high-velocity impact tests (a) Vertical (θ=0°) (b) Inclined (θ=15° and 30°).

2.2 Experimental results

To investigate the effect of impactor head geometry on the impact behavior of honeycombs, three different head geometries (flat, spherical and conical) with the same diameters were considered. This part of the tests was carried out with a vertical impact angle. The effect of impact angle on the impact behavior of honeycombs was studied at

three different impact angles (θ=0°, θ=15°, θ=30°) adjusted by wedges placed under the test fixture. For this part, the flat-head impactor geometry was considered for the tests. The results of the experimental study are presented in Table 2. The ballistic limit is the minimum collision velocity with which an impactor can completely penetrate the target. Fig. 3 shows the experimental residual velocity versus collision velocity plots.

Table 2
The experimental results of the high-velocity impact test for different impactor head geometries and impact angles.

	Spherical-head		Conical-head		Flat-head θ=0°		Flat-head θ=15°		Flat-head θ=30°	
Pressure (*bar*)	Collision velocity (*m/s*)	Residual velocity (*m/s*)	Collision velocity (*m/s*)	Residual velocity (*m/s*)	Collision velocity (*m/s*)	Residual velocity (*m/s*)	Collision velocity (*m/s*)	Residual velocity (*m/s*)	Collision velocity (*m/s*)	Residual velocity (*m/s*)
2	81.1	51.8	90.17	59.1	55.8	48.6	55.8	45.7	55.8	43.3
3	89.02	75.2	98.98	83.8	86.3	81.2	86.3	76.4	86.3	72.2
4	112.1	98.8	124.64	110.3	109.5	107.3	109.5	96.8	109.5	94.6
5	125.54	105.4	139.58	121.5	121.7	116.3	121.7	110.5	121.7	108.5
6	135.4	131.9	150.5	133.5	133.6	127.1	133.5	120	133.5	119.1

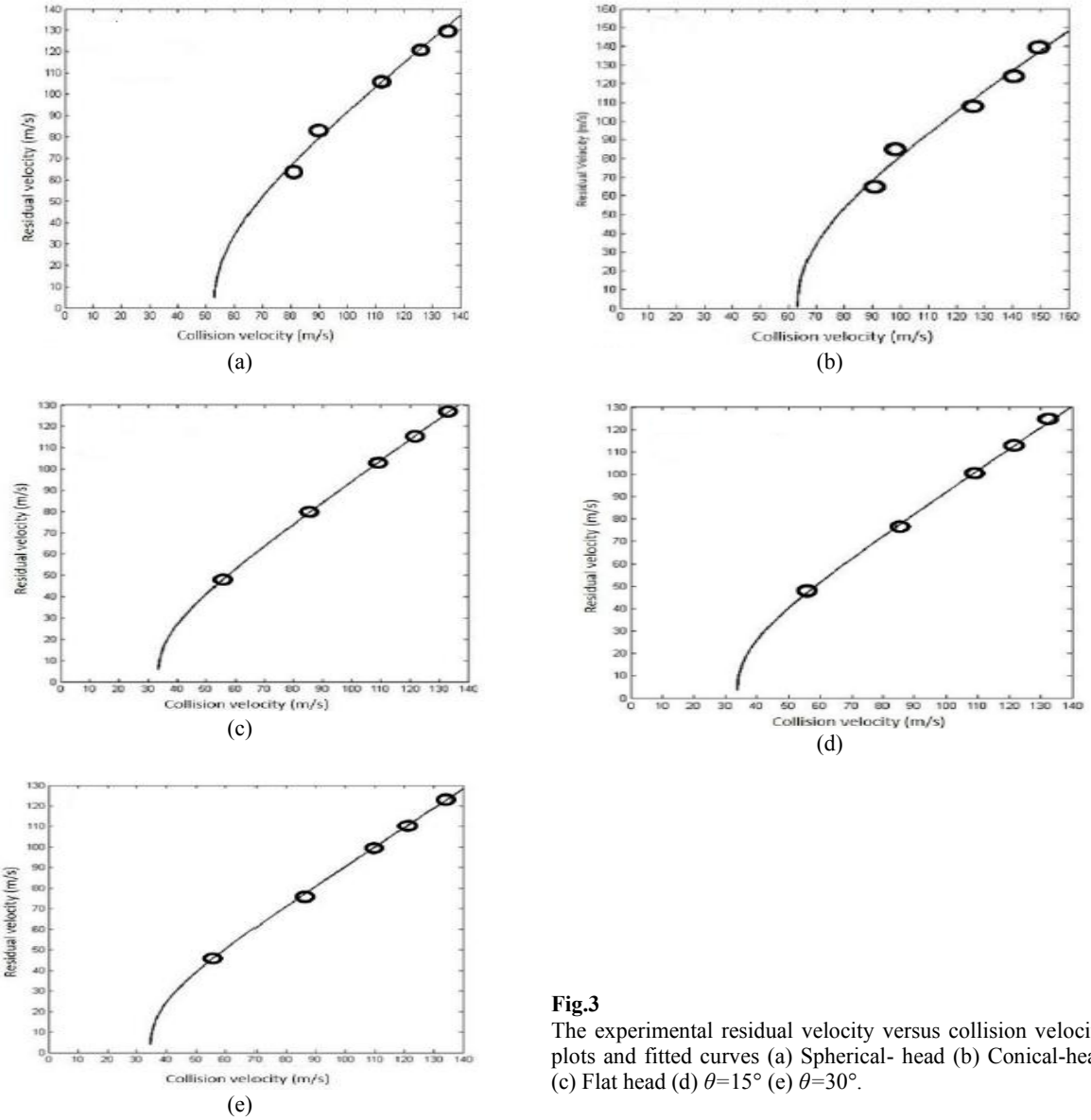

Fig.3
The experimental residual velocity versus collision velocity plots and fitted curves (a) Spherical- head (b) Conical-head (c) Flat head (d) θ=15° (e) θ=30°.

To calculate the ballistic limit velocity, the analytical model proposed by Recht and Ipson [23] was used. Therefore, Eq.(1) was fitted using the least-square method to the experimental residual velocity versus collision velocity data points for different impactor geometries and different impact angles.

$$V_{res} = a(V_i^{\,p} - V_{bl}^{\,p})^{\frac{1}{p}},\ a = \frac{m_p}{m_{pl} + m_p},\ p = 2 \tag{1}$$

In Eq.(1), V_{res} is the residual velocity, V_i is the collision velocity, V_{bl} is the ballistic limit velocity and a and p are two coefficients, m_p is the mass of projectile and m_{pl} is the mass of the part detached from the target. The solid lines in Fig. 2 show the best fitted curves based on the analytical model (Eq.(1)).

The energy absorption of honeycombs in the course of impact loading was calculated using Eq. (2).

$$E_{abs} = \frac{1}{2} m \left(V_i^{\,2} - V_{res}^{\,2} \right) \tag{2}$$

where E_{abs} is absorbed energy, m is the mass of impactor, V_i is the collision velocity and V_{res} is the residual velocity. Fig. 4 shows the experimental ballistic limit velocities and the average absorbed energies for different impactor head geometries and impact angles. The average absorbed energy was the average of the absorbed energies for five different collision velocities.

As can be seen in Fig. 4 the ballistic limit velocity obtained for the flat-head impactor was 55.8% and 54.5% lower than the ballistic limit velocities obtained for the impactors with conical and spherical-head, respectively. This shows the significant influence of the impactor head geometry on the impact behavior of honeycomb. The absorbed energy for the conical-head impactor is 413% and 5.9% more than the flat and spherical geometries, respectively. On the other hand, the ballistic limit velocity of the inclined target with θ=30° was 14% and 28.8% more than the impact angles of θ=15° and θ=0°, respectively. Similarly, the amount of the absorbed energy for the honeycomb fixed at θ=30° was 30.3% and 66.3% higher than that for the impact angles of θ=15° and θ=0°, respectively, signifying the effect of impact angle on the impact behavior of honeycombs.

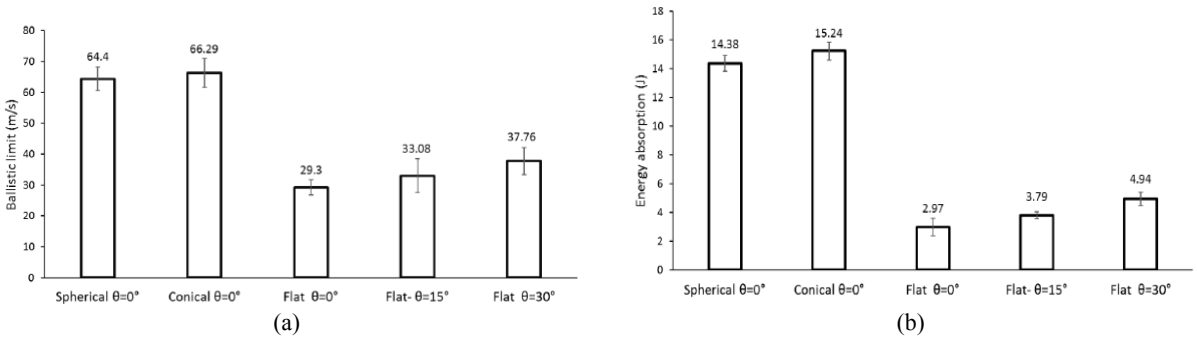

Fig.4
(a) Experimental ballistic limit velocities and (b) Average absorbed energies for different impactor geometries and impact angles.

2.3 Contact surface

The results showed that the honeycomb panels impacted by the projectile with conical-head geometry had the highest ballistic limit velocity and energy absorption, conversely the flat-head impactor caused the lowest ballistic limit velocity and energy absorption for the honeycomb panels. The contact surface of the projectile with target in the course of penetration can be considered as an important factor in the impact behavior of targets. It is obvious that increasing the impact angle increased the contact surface and also the impactor geometry can influence the contact surface.

The contact surface of impactor with target for the conical-head projectile with a cone angle of 60° was more than the spherical and flat-head projectiles. This can be considered as the justification of the effects of the impactor geometry and impact angle on the impact behavior of the honeycombs. Similarly, by increasing the impact angle,

the contact surface of honeycomb and impactor increased and that led to an increase in friction and energy absorption in honeycomb.

2.4 Failure mechanisms

The collision of the impactor to the target generates a stress wave propagating through the target [24]. The collision of impactor induces damages on the target that can be measured after the impact test. The damaged areas of honeycomb panels for different conditions are shown in Fig. 5. The induced damages can reduce the resistance of target against the subsequent impacts.

As can be seen in Fig.5, the damaged area of honeycomb impacted by conical-head impactor was more than the other specimens. By comparison between the size of the damaged area and absorbed energies of different specimens reveals that there was a direct relationship between the size of the damaged area and absorbed energy. The higher amount of the contact surface and friction force led to stronger stress wave and wider damage.

It was found out that different geometries of projectiles imposed different failure mechanisms. For the flat-head impactor, the main failure modes were shear and bending resulted in plugging, petaling and aluminum rapture damage mechanisms as shown in Fig. 6. By comparing the mass of honeycomb panels before and after the impact test, it was found out that a piece of honeycomb was detached from the panel named as plug. In contrast, there was no plug for the conical and spherical-head projectiles, because the failure modes in these cases were bending, tensile and bulging failure mechanisms.

The elastic and plastic deformations of aluminum were two failure mechanisms affecting the absorbed energy [25]. The ability of aluminum in experiencing more plastic deformation, in the course of impact loading, provides high resistance against impact loading as shown in Fig. 7.

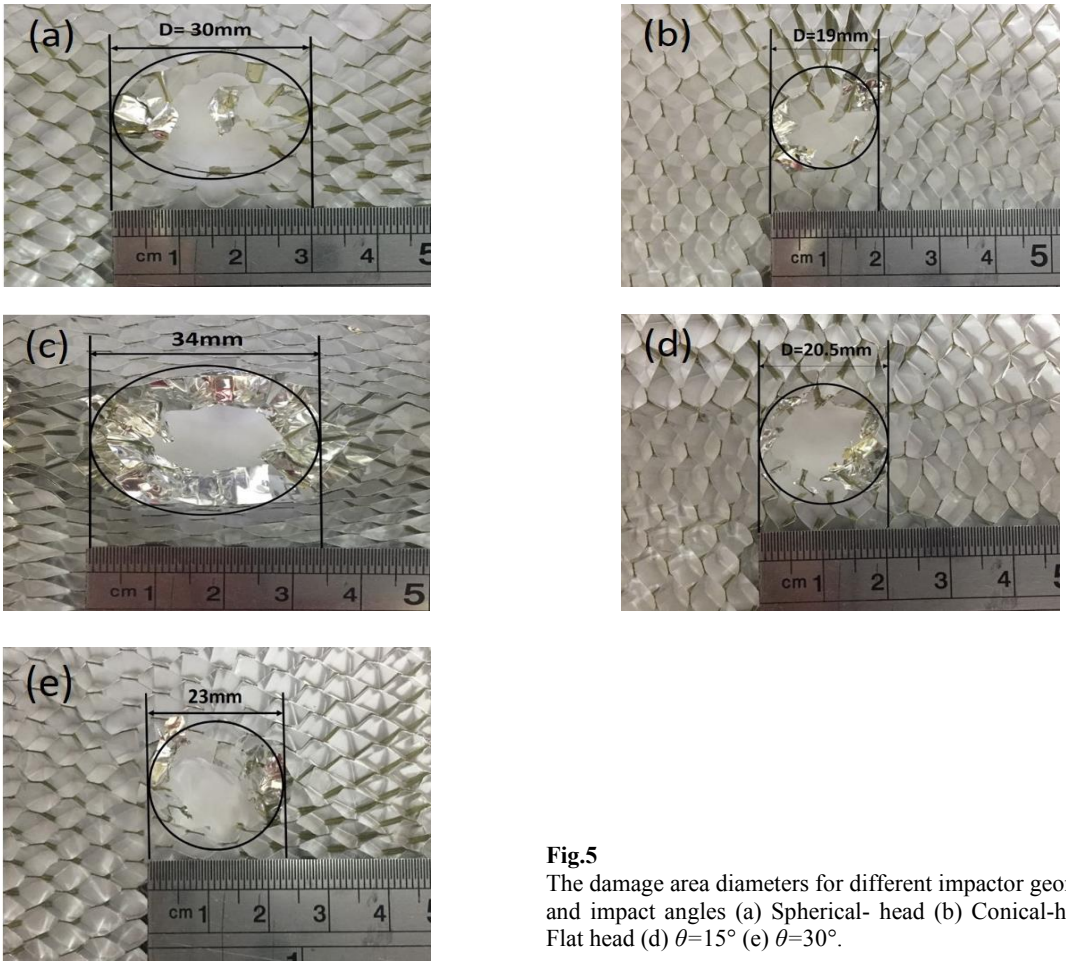

Fig.5
The damage area diameters for different impactor geometries and impact angles (a) Spherical- head (b) Conical-head (c) Flat head (d) θ=15° (e) θ=30°.

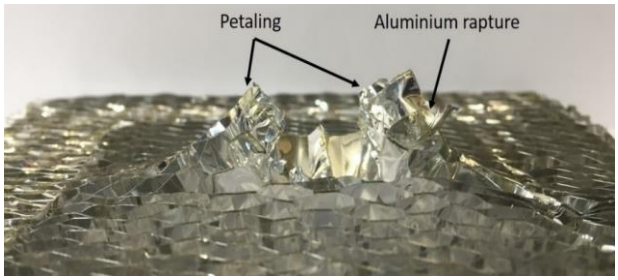

Fig.6
Petaling and aluminum rapture failure mechanisms induced by the flat-head impactor.

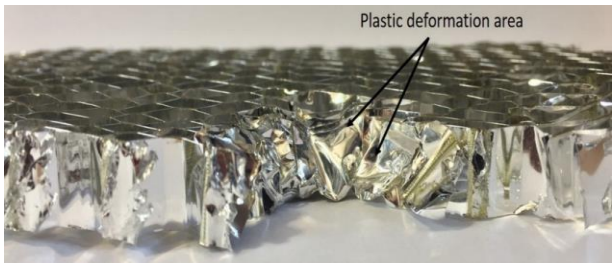

Fig.7
The plastic deformation in honeycomb induced by impact loading.

3 NUMERICAL MODELING

3.1 Finite element model

The high velocity impact test on honeycomb panels was simulated using the LS-Dyna finite element code. The geometrical and finite element models were developed using FEMB as a preprocessor software. Lagrangian elements were used for finite element modeling. Moreover, to reduce the CPU time, the elements around the impacted region were considered fine while the elements far from this region were considered relatively coarse. A mesh sensitivity study was undertaken and the element size close to the impacted region was considered as $0.33\times0.33\times0.5$ mm^3, while the element size far from the impacted zone was considered as $1\times2\times0.5$ mm^3. Fig. 8 shows the finite element model used for the honeycomb panels. Fig. 9 shows the mesh sensitivity results for different projectile geometries.

The impactor was considered as rigid body with the elements larger than those of the honeycomb structure. Fig. 10 shows the finite element models of the impactors. The honeycomb plate was clamped (i.e. the rotational and displacement degrees of freedom of the peripheries of honeycomb plate was restricted) as shown in Fig. 11. The Johnson-Cook material model was employed for modeling the honeycomb panels and the rigid elements were used for the impactor. The material properties and Johnson-Cook parameters of aluminum 1110 used in this study are listed in Table 3 [26].

Table 3
Material properties and Johnson-Cook parameters for aluminum 1110.

$\rho\ (kg/m^3)$	2750
$E(GPa)$	70
m	0.3
$T_m\ (K)$	893
$T_g\ (K)$	293
$A\ (MPa)$	215
$B\ (MPa)$	280
n	0.404
C	0.0085
$\dot{\varepsilon}_0 = (s^{-1})$	5×10^{-4}
m	0.859
$d1$	0.0261
$d\ 2$	0.263
$d\ 3$	0.349
$d\ 4$	0.147
$d\ 5$	16.8

Furthermore, the CONTACT eroding surface to surface algorithm was used for modeling the contact between honeycomb and impactor. Moreover, the CONTACT automatic surface to surface algorithm was used to avoid the collapse of elements.

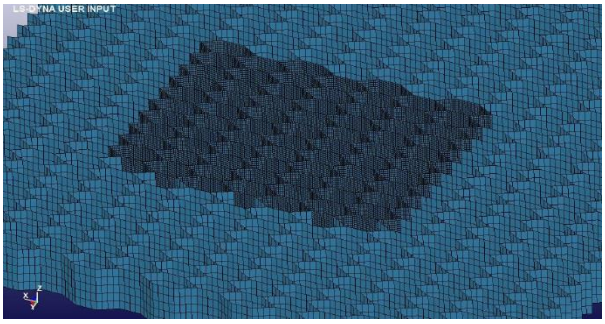

Fig.8
The finite element model of the honeycomb panel.

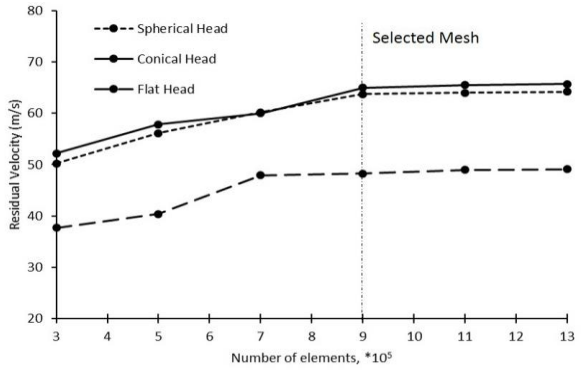

Fig.9
Mesh sensitivity results for different projectile geometries.

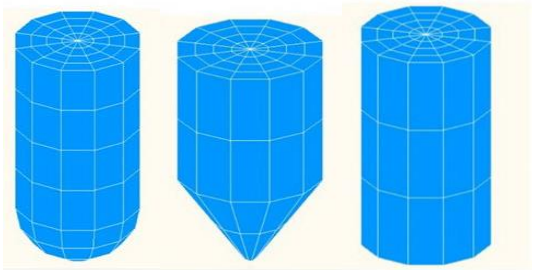

(a) (b) (c)

Fig.10
The finite element models of the impactors with different geometries (a) Spherical-head (b) Conical-head (c) Flat-head.

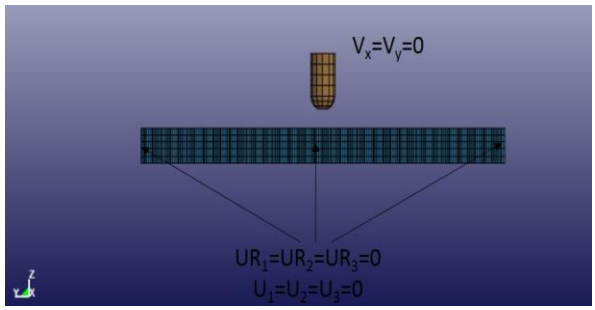

Fig.11
The boundary conditions used in numerical model.

3.2 Model validation

To validate the numerical results, the numerical and experimental results were compared. The residual velocity, ballistic limit and energy absorption were considered for validation.

The residual velocities obtained from the numerical simulation of high-velocity impact loading on honeycombs together with the percentage differences between the numerical and experimental residual velocities are presented in Table 3. As can be seen in Table 4, the average percentage difference between the experimental and numerical residual velocities was 4.91% indicating a reasonable correlation between the experimental and numerical results.

Table 4
Comparison between the numerical and experimental residual velocities.

Pressure (*bar*)	Spherical-head		Conical-head		Flat-head θ=0°		Flat-head θ=15°		Flat-head θ=30°	
	Collision velocity (*m/s*)	Residual velocity (*m/s*) (% difference)	Collision velocity (*m/s*)	Residual velocity (*m/s*) (% difference)	Collision velocity (*m/s*)	Residual velocity (*m/s*) (% difference)	Collision velocity (*m/s*)	Residual velocity (*m/s*) (% difference)	Collision velocity (*m/s*)	Residual velocity (*m/s*) (% difference)
2	81.1	63.72 (+23)	90.17	65.01 (+10)	55.8	48.24 (-0.73)	55.8	47.3 (+3.5)	55.8	45.9 (+6)
3	89.02	83.39 (+10.9)	98.98	85.3 (+1.78)	86.3	79.66 (-1.89)	86.3	77.31 (+1.18)	86.3	76.94 (+6.56)
4	112.1	106.61 (+7.9)	124.64	108 (-2.08)	109.5	103.39 (-3.64)	109.5	100.36 (+3.67)	109.5	98.69 (+4.32)
5	125.54	120.9 (+14.7)	139.58	123.8 (+1.89)	121.7	115.5 (-0.68)	121.7	112.99 (+2.25)	121.7	110.89 (+2.2)
6	135.4	129.9 (-1.5)	150.5	140.2 (+5)	133.6	127.1 (-0.01)	133.5	124.95 (+4.12)	133.5	122.81 (+3.11)

The calculated ballistic limit and energy absorption using Eq.(1) and Eq.(2) for different impactor geometries and impact angles based on the results achieved from the numerical modeling are presented in Table 5.

Table 5
The numerical ballistic limit velocities and average absorbed energies for different impactor geometries and impact angles.

	Ballistic limit (*m/s*)(% difference)	Energy absorption (*J*)(% difference)
Spherical-head	52.8 (-18)	9.67 (-32.7)
Conical-head	63.35 (-4.4)	13.92 (-8.6)
Flat-head θ=0°	33.46 (+14.2)	3.88 (+30.6)
Flat-head θ=15°	33.7 (+1.8)	3.94 (+3.9)
Flat-head θ=30°	34.53 (-8.5)	4.13 (-16.4)

Again reasonable correlation was obtained between the experimental and numerical ballistic limit velocities and absorbed energies. The average difference percentages of 9.39% and 18.44% relative to the experimental results were obtained for the ballistic limit velocity and energy absorption, respectively.

3.3 Numerical impact damage

The induced damages and deformations occurred due to impact loading can be predicted using the numerical model. Fig.12 compares the damaged area diameters derived from the experimental tests and numerical modeling. The predicted damaged area sizes were in a reasonable correlation with the experimental results. In all simulations, the predicted damaged area was obtained less than the corresponding experimental result.

3.4 Penetration time

Fig. 13 shows the time over which the impactor penetrates. The velocity versus time curves are shown in Fig. 13 for the impact tests with a pressure of 6 *bar*. As can be seen in Fig. 13, after passing the projectile through the target, the velocity remained fixed and this velocity was considered as the projectile residual velocity. The penetration time of impactor with the conical-head and an impact angle of θ=30° was obtained more than the other cases.

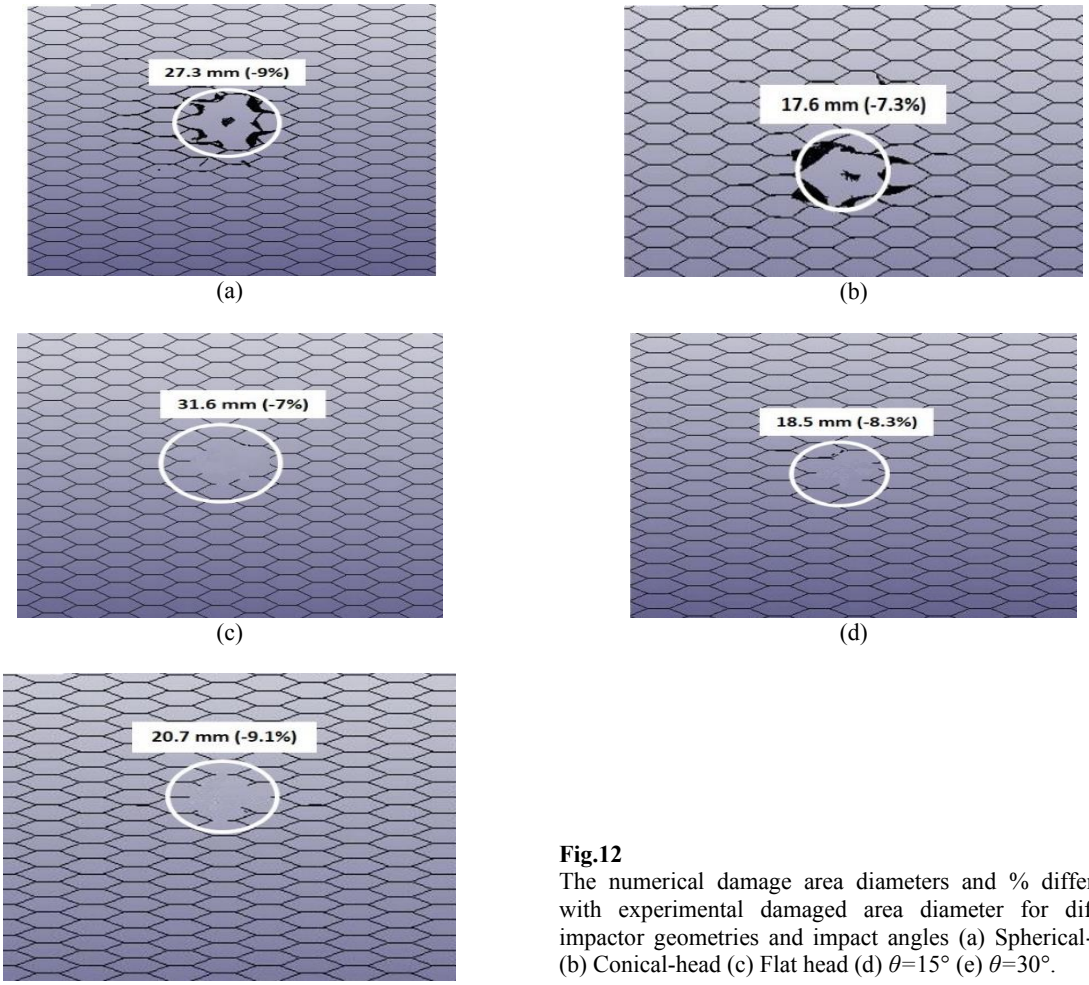

Fig.12
The numerical damage area diameters and % differences with experimental damaged area diameter for different impactor geometries and impact angles (a) Spherical- head (b) Conical-head (c) Flat head (d) θ=15° (e) θ=30°.

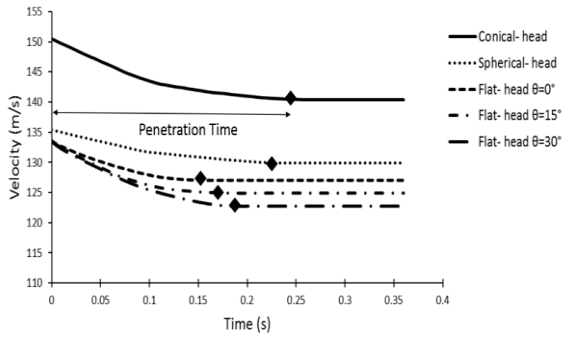

Fig.13
The numerical penetration time of impactors.

4 CONCLUSION

The effect of impactor head geometry and the impact angle on the impact resistance of honeycombs were studied experimentally and numerically. The honeycomb panels were subjected to high-velocity impact loading using a gas-gun test machine and three different impactor head geometries of flat, spherical and conical and three different impact angles of 0°, 15° and 30° were considered. The experimental tests were simulated using the LS-DYNA finite element code. The energy absorption, the ballistic limit velocity, the penetration time and the damaged area size were considered as the impact test outputs. The results of the experimental tests indicated that the ballistic limit and

absorbed energy obtained for the flat-head impactor were considerably lower than those for the other geometries and the honeycomb with θ=30° had the highest value of ballistic limit velocity and absorbed energy. An acceptable correlation was obtained between the experimental and numerical results. Comparison between the damaged areas showed that the honeycomb panel with the larger damaged area experienced higher energy absorption. It was found out that the impactor geometry and impact angle influenced the contact surface of impactor and honeycomb and that changed the energy absorption and penetration time. On the other hand, different impactor head geometries resulted in different combinations of failure mechanisms of petaling, plugging, plastic deformation and aluminum rapture influencing the energy absorption and impact behavior of honeycomb panels.

REFERENCES

[1] Zhang X., Zhang H., Wen Z., 2014, Experimental and numerical studies on the crush resistance of aluminum honeycombs with various cell configurations, *International Journal of Impact Engineering* **66**: 48-59.

[2] Galehdari S.A., Khodarahmi H., Atrian A., 2017, Design and analysis of graded honeycomb shock absorber for increasing the safety of passengers in armored vehicles exposed to mine explosion, *Journal of Solid Mechanics* **9**(2): 370-383.

[3] Zhou Q., Mayer R.R., 2002, Characterization of aluminum honeycomb material failure in large deformation compression, shear, and tearing, *Journal of Engineering Materials and Technology* **124**(4): 412-420.

[4] Fleck N.A., Deshpande V.S., 2004, The resistance of clamped sandwich beams to shock loading, *Journal of Applied Mechanics* **71**(3): 386-401.

[5] Yahaya M.A., Ruan D., Lu G., Dargusch M.S., 2015, Response of aluminium honeycomb sandwich panels subjected to foam projectile impact–An experimental study, *International Journal of Impact Engineering* **75**: 100-109.

[6] Zhang Q.N., Zhang X.W., Lu G.X., Ruan D., 2018, Ballistic impact behaviors of aluminum alloy sandwich panels with honeycomb cores: An experimental study, *Journal of Sandwich Structures & Materials* **20**(7): 861-884.

[7] Hassanpour Roudbeneh F., Liaghat G., Sabouri H., Hadavinia H., 2018, Experimental investigation of impact loading on honeycomb sandwich panels filled with foam, *International Journal of Crashworthiness* **24**: 119-210.

[8] Sun G., Chen D., Wang H., Hazell P.J., Li Q., 2018, High-velocity impact behaviour of aluminium honeycomb sandwich panels with different structural configurations, *International Journal of Impact Engineering* **122**: 119-136.

[9] Xu S., Beynon J.H., Ruan D., Lu G., 2012, Experimental study of the out-of-plane dynamic compression of hexagonal honeycombs, *Composite Structures* **94**(8): 2326-2336.

[10] Zhao H., Gary G., 1998, Crushing behaviour of aluminium honeycombs under impact loading, *International Journal of Impact Engineering* **21**(10): 827-836.

[11] Baker W.E., Togami T.C., Weydert J.C., 1998, Static and dynamic properties of high-density metal honeycombs, *International Journal of Impact Engineering* **21**(3): 149-163.

[12] Liaghat G.H., Nia A.A., Daghyani H.R., Sadighi M., 2010, Ballistic limit evaluation for impact of cylindrical projectiles on honeycomb panels, *Thin-Walled Structures* **48**(1): 55-61.

[13] He W., Yao L., Meng X., Sun G., Xie D., Liu J., 2019, Effect of structural parameters on low-velocity impact behavior of aluminum honeycomb sandwich structures with CFRP face sheets, *Thin-Walled Structures* **137**: 411-432.

[14] Guan G.Y., Liu Z.C., Hu G., Zhang Y., 2017, Experimental study of the effect of aluminum panel thickness on flexural properties of nomex honeycomb sandwich structure subjected to low velocity impact, *Journal of Experimental Mechanics* **2017**(4): 14.

[15] Yamashita M., Gotoh M., 2005, Impact behavior of honeycomb structures with various cell specifications—numerical simulation and experiment, *International Journal of Impact Engineering* **32**(1-4): 618-630.

[16] Wu Y., Meng L.Q., Zhou Z.W., Shu X.F., 2011, Deformation mode analysis of nomex honeycomb sandwich beam subjected to impact loading, *Journal of Experimental Mechanics* **2011**(6): 17.

[17] Qi C., Remennikov A., Pei L.Z., Yang S., Yu Z.H., Ngo T.D., 2017, Impact and close-in blast response of auxetic honeycomb-cored sandwich panels: Experimental tests and numerical simulations, *Composite Structures* **180**: 161-178.

[18] Hosseini M., Khalili S.M.R., 2013, Analytical prediction of indentation and low-velocity impact responses of fully backed composite sandwich plates, *Journal of Solid Mechanics* **5**: 278-289.

[19] Gunes R., Arslan K., 2016, Development of numerical realistic model for predicting low-velocity impact response of aluminium honeycomb sandwich structures, *Journal of Sandwich Structures & Materials* **18**(1): 95-112.

[20] Galehdari S.A., Kadkhodayan M., Hadidi-Moud S., 2015, Low velocity impact and quasi-static in-plane loading on a graded honeycomb structure; experimental, analytical and numerical study, *Aerospace Science and Technology* **47**: 425-433.

[21] Aktay L., Johnson A.F., Kröplin B.H., 2008, Numerical modelling of honeycomb core crush behavior, *Engineering Fracture Mechanics* **75**(9): 2616-2630.

[22] Li L., Zhao Z., Zhang R., Han B., Zhang Q., Lu T.J., 2019, Dual-level stress plateaus in honeycombs subjected to impact loading: perspectives from bucklewaves, buckling and cell-wall progressive folding, *Acta Mechanica Sinica* **35**(1): 70-77.

[23] Recht R., Ipson T.W., 1963, Ballistic perforation dynamics, *Journal of Applied Mechanics* **30**(3): 384-390.

[24] Shariyat M., Moradi M., Samaee S., 2012, Nonlinear finite element eccentric low-velocity impact analysis of rectangular laminated composite plates subjected to in-phase/anti-phase biaxial preloads, *Journal of Solid Mechanics* **4**: 177-194.

[25] Talebi S., Sadighi M., Aghdam M.M., 2019, Numerical and experimental analysis of the closed-cell aluminium foam under low velocity impact using computerized tomography technique, *Acta Mechanica Sinica* **35**(1): 144-155.

[26] Wang J., Hu X., Yuan K., Meng., Li P., 2019, Impact resistance prediction of superalloy honeycomb using modified Johnson–Cook constitutive model and fracture criterion, *International Journal of Impact Engineering* **131**: 66-77.